

RSC Advances



This is an *Accepted Manuscript*, which has been through the Royal Society of Chemistry peer review process and has been accepted for publication.

Accepted Manuscripts are published online shortly after acceptance, before technical editing, formatting and proof reading. Using this free service, authors can make their results available to the community, in citable form, before we publish the edited article. This *Accepted Manuscript* will be replaced by the edited, formatted and paginated article as soon as this is available.

You can find more information about *Accepted Manuscripts* in the [Information for Authors](#).

Please note that technical editing may introduce minor changes to the text and/or graphics, which may alter content. The journal's standard [Terms & Conditions](#) and the [Ethical guidelines](#) still apply. In no event shall the Royal Society of Chemistry be held responsible for any errors or omissions in this *Accepted Manuscript* or any consequences arising from the use of any information it contains.

1 **Responses of ammonia-oxidizing bacteria community composition to**
2 **temporal changes in physicochemical parameters during food waste**
3 **composting**

4
5 **Shanshan Shi,^a Dexun Zou,^b Qunhui Wang,^{* a, c} Xunfeng Xia,^d Tianlong Zheng,^a Chuanfu Wu,^a Ming**
6 **Gao^e**

7
8 *^a Department of Environmental Engineering, University of Science and Technology Beijing, Beijing 100083,*
9 *P. R. China*

10 *^b Centre for Resource and Environmental Research, Beijing University of Chemical Technology, Beijing*
11 *100029, P. R. China*

12 *^c Beijing Key Laboratory on Resource-oriented Treatment of Industrial Pollutants, University of Science and*
13 *Technology Beijing, Beijing 100083, P. R. China*

14 *^d Laboratory of Water Environmental System Engineering, Chinese Research Academy of Environmental*
15 *Science, Beijing 100012, P. R. China*

16 *^e Laboratory of Microbial Technology, Division of Systems Bioengineering, Department of Bioscience and*
17 *Biotechnology, Faculty of Agriculture, Graduate School, Kyushu University, 6-10-1 Hakozaki, Higashi-ku,*
18 *Fukuoka 812-8581, Japan*

19

20 ***Corresponding author**

21 **E-mail: wangqh59@sina.com**

22 **Tel/Fax: +86-(10)-62332778**

23 **Abstract**

24 Chemoautotrophic ammonia-oxidizing bacteria (AOB) serve an important function in ecological nitrogen
25 transformation because of their great potential to alleviate ammonia emissions during aerobic composting.
26 However, studies on the influence of specific environmental factors on AOB community dynamics in the
27 food waste composting field are scarce. Hence, this study aimed to identify and prioritize some
28 environmental parameters that affect AOB community composition during food waste composting. The
29 composition and diversity of the AOB community were determined using polymerase chain
30 reaction-denaturing gradient gel electrophoresis (PCR-DGGE). Relationships between the obtained
31 parameters and AOB community composition were simultaneously evaluated by multivariate analysis.
32 Phylogenetic analysis indicated that large amounts of *Nitrosomonas*-like and *Nitrospira*-like lineages
33 existed in different periods. The *Nitrosomonas europaea/eutropha* were the most dominant AOB species in
34 the thermophilic stage. Redundancy analysis revealed that the dynamics of AOB community was mainly
35 attributed to temporal changes in nitrate and pH of the compost material ($p < 0.05$). Variations (54.7% for
36 AOB species data) were statistically explained by nitrate and pH, suggesting that these parameters were the
37 most likely to influence, or be influenced by AOB community composition, and may further influence
38 nitrogen cycle in the food waste composting ecosystem.

39

40 **Keywords:** Food waste composting; Ammonia-oxidizing bacteria (AOB); Community composition;
41 Multivariate analysis

42

43 1. Introduction

44 Food waste is the largest component of household waste in China, more than 60 million tons of which are
45 being produced each year, accounting for about 40%–50% weight of the total household waste. Food waste
46 is usually transported to a landfill site for disposal.¹ However, various problems, such as putrid smell and
47 leachate pollution of underground waters, are encountered. Incineration is another method for disposal but is
48 not suitable for use because the low calorific value and high water content of food waste require high energy
49 input. In addition, incineration causes air and environmental pollution.²

50 To date, composting is a promising alternative treatment technique that enables the reuse of valuable
51 organic contents of food waste.^{3,4} However, high concentration of organic nitrogen in food waste is readily
52 converted into ammonia-N ($\text{NH}_4^+\text{-N}$) by microorganisms. In addition, an alkaline pH may lead to substantial
53 losses of nitrogen as gaseous ammonia (NH_3) during the composting process. The emission of NH_3
54 contributes to air pollution and reduces the fertilizing value of the compost.⁵ Ammonia-oxidizing bacteria
55 (AOB) serve an important role in nitrification during composting because it can oxidize ammonia and reduce
56 the emission of gaseous ammonia (NH_3).⁶ Moreover, the function of AOB to the nitrogen cycle has gained
57 increasing attention in research on the basis of the fact that ammonia oxidation might be the rate-limiting
58 step of nitrification.⁷ Therefore, the underlying community succession of AOB and their responses to
59 composting conditions need to be deeply understood.

60 AOB are now widely accepted as the major agents of nitrification. A number of AOB populations have
61 been detected in various types of composting materials including commercial biofertilizer products. Several
62 clusters including the genera *Nitrosospira* and *Nitrosomonas* are present among different kinds of
63 composting materials, such as mushroom cultivation and pig or chicken manure.⁸ Jarvis et al. detected
64 *Nitrosomonas* in the thermophilic stage and *Nitrosospira* in the maturation phase of household waste
65 composting.⁹ Maeda et al. also detected *Nitrosomonas* throughout the process, especially from the surface

66 layer of a cattle manure composting pile.¹⁰ Innerebner et al. found that the clone library from the sewage
67 sludge compost was dominated by *Nitrosospira*-like sequences.¹¹ Food waste as raw material is now widely
68 used in composting; however, few studies on the composition and diversity of AOB community have been
69 reported.

70 AOB community dynamics may be influenced by various environmental parameters, including
71 temperature, pH, ammonium concentration, and organic matter. Yamamoto et al. reported that pile
72 temperature affected the AOB community structure.¹² They reported that a member of the *Nitrosomonas*
73 *europaea* cluster dominated the community at high-temperature stage. Another study showed that different
74 ammonia oxidizer phylotypes were selected in soils with different pH.¹³ Furthermore, another study
75 demonstrated that AOB population size was significantly greater in annually fertilized soil than that in
76 unfertilized, suggesting that ammonium fertilization has a long-term effect on AOB population size.¹⁴ Other
77 researchers observed that the organic matter affected the nitrification rate and AOB community composition
78 in the wastewater treatment reactor.¹⁵ These reports helped us further understand that environmental
79 parameters cause the actual composition of AOB community. However, few studies on the effects of
80 temporal changes in physicochemical parameters on the community structure of AOB in the food waste
81 composting field have been conducted.

82 An improved understanding of the different environmental parameters and their combinations that affect
83 community composition of AOB, as well as their responses to environmental change is essential for the
84 prediction and control of the ecosystem functions in food waste composting. Therefore, the objectives of this
85 research were two-fold: firstly, investigated the diversity and community structure of AOB during different
86 phases of the food waste composting by using polymerase chain reaction-denaturing gradient gel
87 electrophoresis (PCR-DGGE); and secondly, the influence of the physicochemical parameters, such as
88 temperature, pH, ammonium concentration and organic matter which would significantly affect the AOB

89 community structure, were prioritized using multivariate approach. We suppose that our study will play a
90 guiding role for the practical application of food composting.

91 **2. Material and methods**

92 **2.1 Lab-scale composting reactor**

93 A schematic of the lab-scale composting reactor is illustrated in Fig. 1. A 75 L stainless steel cylindrical
94 reactor (inner diameter: 30 cm, length: 50 cm, net volume: 75 L, filling height of the compost: 45 L) with
95 insulation was used for the composting study. High density polyurethane was employed as the outer layer of
96 the thermal insulation materials to prevent heat loss. An agitator shaft with agitating blades was horizontally
97 mounted inside the reactor for intermittent mixing. An aeration tube was also installed at the bottom of the
98 composting reactor to maintain aerobic condition. The air was supplied using an air pump at a flow rate of
99 $0.1 \text{ m}^3 \cdot \text{min}^{-1} \cdot \text{m}^{-3}$. On top of the reactor, an exhaust air pipe was connected to a water-cooling device where
100 water vapor can be condensed, collected, and sent back to the reactor to maintain the moisture content of the
101 composts. A thermocouple was also placed at the middle-level of the reactor to continuously monitor the
102 temperature variation using a controller. Ammonia gas released during composting was captured by an
103 ammonia sensor. The exhaust air passed through a sodium hydroxide solution for the absorption of carbon
104 dioxide before the final emission.

105 **2.2 Raw material and composting process**

106 Food waste from the dining room of the University of Science and Technology of Beijing, Beijing City,
107 China was used as raw material. The mushroom residue used as a bulking agent because of its high porosity
108 and low moisture content was collected from a local edible mushroom factory in Fangshan District in Beijing.
109 These materials were cut into pieces of approximately 1 cm. The physicochemical characteristics of the
110 initial raw materials are listed in Table 1.

111 Carbon (C), and nitrogen (N) are the primary nutrients required by the microorganisms involved in

112 composting. Microorganisms use carbon for both energy and growth, while nitrogen is essential for protein
113 production and reproduction. The C/N ratio (i.e., the ratio of carbon to nitrogen) of 25:1 to 30:1 is considered
114 the ideal range for active composting, since the microorganisms require 30 parts of C per unit of N.¹⁶ High
115 C/N ratios make the process very slow as there is an excess of degradable substrate for the microorganisms.
116 But with a low C/N ratio there is an excess of N per degradable C and inorganic N is produced in excess and
117 can be lost by ammonia volatilization or by leaching from the composting mass. As shown in Table 1, food
118 waste had relative low C/N ratios, but high moisture content. Therefore, addition of mushroom residue with
119 high C/N ratio as a bulking agent was beneficial for adjusting the initial C/N ration to the range of 25:1 to
120 30:1. The initial pH was adjusted to about 6.5 and moisture content was adjusted to 60% using deionized
121 water; 45 L of the mixture was then placed into the 75 L lab-scale composting reactor. Moisture content was
122 maintained at 50% using the condensed water sent back to the reactor. Deionized water was supplemented
123 when the moisture content can no longer be maintained by the water being sent back to the reactor.
124 Composting was carried out under aerobic conditions for 15 days. Subsamples were randomly collected at
125 three different depths. Samples were pooled, mixed, and then divided into three parts, where one part was
126 stored at $-80\text{ }^{\circ}\text{C}$ and the other two were air-dried immediately and stored at $4\text{ }^{\circ}\text{C}$.

127 **2.3 Physicochemical analysis of the composting samples**

128 Temperature was continuously recorded by a computer connected to the reactor through a sensor inserted
129 into the middle of the composting materials; environmental temperature was also measured at the same time.
130 The pH level was measured by a compound electrode (PE-10, Sartorius, Germany) dipped into a solution
131 of 5 g of fresh sample and 50 mL of deionized water. Moisture content was determined by drying the fresh
132 sample in a drying oven at $105\text{ }^{\circ}\text{C}$ until constant weight was achieved. Organic matter content (OM) was
133 quantified by weight loss after ignition in a furnace at $550\text{ }^{\circ}\text{C}$.¹⁷ Concentrations of nitrate (NO_3^- -N) and
134 ammonium (NH_4^+ -N) were extracted with 2 M KCl and measured using an AutoAnalyzer (AA3, Bran and

135 Luebbe, Germany).

136 **2.4 DNA extraction and PCR-DGGE**

137 Total genomic DNA was extracted according to the method described previously by Yang et al.¹⁸ DNA
138 extracts were 10-fold diluted before PCR to overcome the possible inhibition by humic acids. The extracted
139 DNA was purified, dissolved in 100 μ L of TE buffer, and then stored at -20 °C before use.

140 A nested PCR approach was used to amplify ammonia-oxidizer specific 16S rRNA for DGGE.¹⁹ The
141 first-round of PCR was conducted using the AOB-specific primer pair CTO189f-GC and CTO654r, which
142 was amplified as a 465 bp fragment.²⁰ The product from this round of PCR was then used as template DNA
143 for the second-round of PCR carried out using universal primers F338-GC and R518.²¹ PCR mixtures diluted
144 to a final volume of 25 μ L contained 12.5 μ L $2 \times$ *EasyTaq* PCR SuperMix (TransGen Biotech, Beijing,
145 China), 0.5 μ M of each primer, and 1 μ L of 10-fold diluted DNA. PCR reactions were performed on a
146 MyCycler Thermal Cycler (Bio-Rad, USA) as previously described.¹⁹ All PCR amplicons were examined by
147 electrophoresis in 1.0% (wt/vol) agarose with ethidium bromide staining to confirm the product size.

148 The nested PCR amplicons were separated by DGGE using a DCode™ Universal Detection System
149 (Bio-Rad, USA) according to the instructions of the manufacturer. Approximately 20 μ L of each PCR
150 product was loaded onto an 8% (w/v) polyacrylamide gel (acrylamide : bisacrylamide = 37.5 : 1) with a
151 denaturant gradient of 30%–60% for AOB (100% denaturant contains 7M urea and 40% deionized
152 formamide). Electrophoresis was then conducted at 60 °C in $1 \times$ Tris-acetate-EDTA buffer at 110 V for 12 h.
153 After DGGE, the gels were stained with 1:10,000 SYBR green I for 30 min, and then scanned with a
154 Bio-Rad image scanner. Band intensity and position data were analyzed using the software Quality One v4.6
155 (Bio-Rad, USA).

156 **2.5 Sequencing and phylogenetic analysis**

157 Prominent DGGE bands were excised using sterilized cutter blades and transferred into 40 μ L Milli-Q

158 water, and then incubated overnight at 4 °C. DNA was recovered from the gel by freeze-thawing three times.
159 The eluted DNA from excised DGGE bands were re-amplified with the primer set F338-GC/R518, and the
160 products again were subjected to DGGE to check their migration. The target DNA fragments were then
161 excised and re-amplified using the primer set F338-GC/R518 without the GC-clamp, thus obtaining a pure
162 sample for the cloning and sequencing step. The purified PCR products were cloned into the pGM-T vector
163 (Tiangen Biotech, Beijing, China) and transformed into *Escherichia coli* TOP10 (Tiangen Biotech, Beijing,
164 China). The plasmids of positive colonies were extracted and sequenced.

165 The sequences of the DGGE bands were compared with those available in the National Center for
166 Biotechnology Information (NCBI, <http://blast.ncbi.nlm.nih.gov/Blast.cgi>). GenBank database using the
167 BLAST algorithm. The nucleotides generated in this study and those from the NCBI GenBank database were
168 aligned. A phylogenetic tree was constructed by the neighbor-joining method using Kimura 2-parameter
169 distance, as implemented in MEGA version 5.0. Bootstrap support (> 50%) from 1000 replications is shown
170 at the nodes of the tree.

171 2.6 Statistical analysis

172 Statistical analyses were performed using SPSS version 20.0. Three replicates were used in all parameter
173 analysis. Data presented as the mean values of triplicates and the maximum difference among triplicate
174 results was below 5%. DGGE profiles were converted into matrix data based on the number of bands and
175 their relative intensities among the individual samples using the software Quality One v4.6 (Bio-Rad, USA).

176 Shannon diversity index (H) was calculated by the following equation: $H = -\sum (ni/N) \log(ni/N)$,
177 where ni/N is the community proportion made up by species i (brightness of the band i /total brightness
178 of all bands in the lane).²²

179 The correlation between environmental factors and the AOB community was evaluated by multivariate
180 analysis using Canoco 4.5 software.²³

181 2.7 Nucleotide sequence accession numbers

182 The sequences obtained from the DGGE bands in this study were submitted to GenBank under the
183 accession numbers KJ890593 to KJ890606.

184 3. Results and discussion

185 3.1 Temporal changes in the properties of material during composting

186 Variation of pile temperature during food waste composting is illustrated in Fig. 2a, including the
187 mesophilic phase (days 1–2), thermophilic phase (days 3–9), and cooling phase (days 10–15). Pile
188 temperature rapidly increased in less than three days and reached a thermophilic level ($>50\text{ }^{\circ}\text{C}$), indicating
189 that indigenous microorganisms easily utilize the food waste organic matter. The thermophilic phase that
190 lasted for seven days was necessary to attain proper disinfection of waste materials from animal and plant
191 pathogens.²⁴ After the sharp breakdown of organic matter on the ninth day, the pile temperature decreased
192 gradually and went back to ambient, indicating the end of the composting process. The pH slightly dropped
193 to 6.50 starting on the second day because of the produced organic acids as intermediate by-products of
194 easily degradable organic matter in food waste.²⁵ Following the increase in temperature, the pH value
195 reached its peak on the sixth day as a result of the production of ammonia from the degradation of organic
196 decomposition (Fig. 2b and Fig. 2c). The pH then decreased slightly to 8.2 at the end of the process. Process
197 performance regarding pH is similar to that reported in other runs using the same compost reactor.³ Moisture
198 content was maintained at 50% by periodic watering (Fig. 1b) because it was suitable for aerobic microbial
199 activity.²⁶ Organic matter content decreased from 87.7% to 67.5% during the composting process (Fig. 1b)
200 because labile fractions of the organic matter were mineralized into stable compounds by microbial activities.
201 The increase in ammonium ($\text{NH}_4^+\text{-N}$) concentration from initial 528.1 mg kg^{-1} to the maximal 1142.7 mg
202 kg^{-1} on the sixth day indicates the decomposition of nitrogenous organic compound into ammonia (NH_3).
203 The $\text{NH}_4^+\text{-N}$ concentration decreased because of the NH_3 volatilization and the immobilization by

204 microorganisms. Nitrate (NO_3^- -N) concentration showed a slight increase on the third day and kept a
205 downward trend to 125.2 mg kg^{-1} on the ninth day as high temperature and excessive amount of ammonia
206 inhibited the activity and growth of nitrifying organisms. Nitrate concentration then gradually increased to as
207 high as 445.6 mg kg^{-1} .

208 **3.2 Temporal dynamics of AOB community during food waste composting**

209 DGGE analysis was used to investigate the community structure and identify certain AOB groups present
210 during the different stages of food waste composting. The distribution of the 14 bands (Fig. 3) detected in the
211 DGGE profiles during different phases indicated that AOB composition was dynamic during food waste
212 composting. Most of the bands were ubiquitous but had different relative abundances in different stages, due
213 to the composting environments of different stage was unique, affecting the intrinsic AOB community. The
214 diversity of the AOB community was evaluated using the Shannon diversity index since it is a
215 comprehensive parameter used to evaluate microbial diversity, and considers both numbers and relative
216 intensity of bands. As shown in Table 2, the indices and band number in the samples collected from the
217 mesophilic (days 1–2) and cooling phases (days 10–15) were higher than that of the thermophilic phase
218 (days 3–9). Indigenous ammonia-oxidizing population proliferated in the food waste in ambient temperature
219 because of the relative abundance of easily degradable organic compounds at the beginning of composting.
220 However, the diversity of AOB decreased with increasing temperature because the sensitivity of AOB in
221 these conditions varies from species to species.²⁷ Finally, the diversity indices of AOB increased after the
222 thermophilic phase and reached its peak value on the 12th day of the cooling phase. These results indicate
223 that AOB communities are active in both the mesophilic and cooling phases. This phenomenon is similar to
224 the result of Zhang et al., who reported that AOB were related to ammonia oxidation in the mesophilic and
225 maturation phases.²³ Furthermore, this finding confirmed the reasons for the increase in nitrate concentration
226 during the cooling phase (Fig. 1c).

227 DGGE fragments were carefully excised and sequenced from the DGGE gel to better visualize the
228 temporal dynamics of the AOB communities. Nucleotide sequences obtained were compared with those
229 available in the NCBI database using BLAST. Phylogenetic tree based on AOB nucleic acid sequences is
230 shown in Fig. 4. The majority of the sequences were closely related to ammonia-oxidizing lineages
231 belonging to the β -subclass of the *Proteobacteria*. Nine out of 14 sequences were most similar to the genus
232 *Nitrosomonas*, and five practically belonged to the genus *Nitrospira*.

233 In the thermophilic phase, majority of the sequences (band a, b, c, d, f, and g in Fig. 4) were correlated
234 with those recovered from the sludge, municipal solid waste, and saline rhizospheric soil and were grouped
235 into the *Nitrosomonas europaea/eutropha* cluster.^{28,29} This result was consistent with previous reports
236 showing that the *Nitrosomonas europaea/eutropha* preferred environments with high ammonium and pH.^{9,12}
237 Our results also confirmed that the *N. europaea/eutropha* can tolerate high temperature (Fig. 2a) and high
238 ammonium concentration (Fig. 2c), which may serve an important function in the ammoxidation of food
239 waste composting. On the other hand, bands a, h, i, j, l, and m in the mesophilic phase were affiliated with
240 the *Nitrosomonas* and *Nitrospira* lineage (Fig. 4). Bands a and m particularly dominated over the entire
241 composting period, while other bands appeared only in specific period. It might be because that, as
242 aforementioned, different composting period contains a unique environment, affecting the intrinsic AOB
243 community. The species of band m can better adapt to changing environmental conditions, compared with
244 other species. And this flexibility is important in determining the dynamics of ammonia oxidation during
245 composting.⁹ Furthermore, band m fell within the *Nitrospira* cluster 3, which was also detected in the
246 initial stage of mushroom cultivation composting.⁸ However, this result was inconsistent with the report of
247 Yamamoto where he stated that the difference in species dominance may be attributed to the chemical
248 properties of raw materials.¹² Most of the bands during the cooling phase (bands a, e, f, g, j, k, l, and m in Fig.
249 4) fell into the *Nitrosomonas* cluster 7 and *Nitrospira* cluster 3, suggesting that they co-migrated with the

250 predominant bands from the mesophilic and thermophilic phases. Therefore, these data showed that
251 *Nitrosomonas*-like and *Nitrosospira*-like sequences abundantly existed during the different periods of the
252 process and acted as ammonia oxidizers. Furthermore, dominant AOB species shifted with various
253 environmental parameters.

254 **3.3 Correlations of the environmental parameters with community structures of AOB**

255 Detrended correspondence analysis was performed first to choose between linear or unimodal response
256 models for AOB species.³⁰ In this study, the length of the first ordination axis was 1.915, showing that linear
257 species response models are well-suited for the data analysis. Therefore, the influence of the environmental
258 factors on AOB community (Fig. 5) was investigated by redundancy analysis. The analysis result is shown in
259 Table 3. The first two canonical axes for the AOB DGGE fingerprints explained 41.1% and 28.8% of the
260 variation during the species data, respectively. The 91.2% increase in variation in the species data was
261 explained by all canonical axes. Monte-Carlo permutation tests demonstrated that both the first axis and all
262 axes combined explained the significant amount of variability in the AOB community structure ($p < 0.05$),
263 indicating that environmental variables may have an important role in explaining the variability of the AOB
264 community.

265 This research aimed to identify which among the environmental variables affect AOB community
266 composition. Forward selection was performed to identify the variables that best describe the most influential
267 gradients. Explanatory variables were added until the addition of further parameters failed to significantly
268 improve the model explanatory power ($p < 0.05$). In this procedure, nitrate and pH statistically explained the
269 variation ($p < 0.05$) on the distribution of AOB species data; whereas, the other parameters did not
270 statistically explain the variation ($p > 0.05$). Furthermore, the percentages of variation explained by each of
271 the significant parameters in Table 4 were those without shared variation. Nitrate solely explained 27.3% (p
272 = 0.012) of the variation on the AOB species data, whereas pH explained 21.7% ($p = 0.024$). Meanwhile, the

273 RDA model (i.e., nitrate and pH) statistically explained 54.7% of the variation ($p = 0.002$). These results
274 showed that environmental parameters (i.e., nitrate and pH) and their interactions predominantly affect AOB
275 community composition.

276 Multivariate statistical analysis suggested that nitrate and pH have predominant effect on AOB community
277 composition ($p < 0.05$). The importance of nitrate variation in the AOB community had been highlighted by
278 Zhang et al.²³ Moreover, AOB may serve an important function in nitrification during composting.¹² In our
279 study, *Nitrosomonas*-like and *Nitrosospira*-like ammonia oxidizers of the β -subdivision of class
280 *Proteobacteria* had been detected (Fig. 4). Betaproteobacterial AOB are chemoautotrophic and generate
281 energy from the hydroxylamine oxidation step, the ATP produced is used to fix CO_2 as a carbon source.
282 Therefore, the presence of these AOB indicates that these bacteria oxidize ammonia in the composting
283 process. Accumulation of nitrate in the cooling phase of the composting process (Fig. 2c) reveals that
284 ammonia oxidizers are more active in the food waste compost pile. Environmental conditions are favorable
285 for the AOB activity may affect the net nitrogen balance during the composting process.⁹

286 Another important factor affecting AOB community structure is pH. The presence of low pH values
287 usually coincide with reduced microbial activities.²⁵ In addition, pH affects the chemical form, concentration,
288 and availability of substrates, as well as cell growth and activity.³¹ For example, rates of nitrification and, in
289 particular, ammonia oxidation are significantly reduced in acid soils, whereas higher nitrification rate is
290 found in the alkaline environment.^{32,33} The reduced growth and activity of ammonia oxidizers at low pH is
291 attributed to the exponential reduction in NH_3 availability with decreasing pH, through ionization to NH_4^+ ,
292 decreasing NH_3 diffusion and increasing the requirement for energy-dependent transport of NH_4^+ .³⁴
293 Furthermore, pH affects the AOB community structure. Jarvis and Nugroho reported a selection for the
294 *Nitrosospira* clusters 2 and 4 strains in the acidic compost and neutral soil.^{9,33} Yamamoto et al. indicated that
295 the *N. europaea/eutropha* (cluster 7) have been shown to be favored by high pH and high ammonia

296 conditions.¹² The pH of the food waste composting in this study is basic. Therefore, strong correlations
297 between pH and AOB community activity were observed in our work. The pH of the food waste composting
298 in this study is critical. Strong correlations between pH and AOB community activity were observed in our
299 work. This result revealed that the activity of the AOB could be encouraged through proper control of the pH
300 of the compost during the fermentation process. Consequently, the negative effect to environment due to
301 ammonia emission and nutrient (i.e., fertilization) elevation of the compost by nitrogen conservation could
302 be gained. However, more convincing result could be obtained after demonstrating it in the scale-up
303 composting plant. On the other hand, notwithstanding, no significant relationship was observed between the
304 other environmental parameters and AOB community composition in this work. This result does not imply
305 that those parameters are of no importance in determining the AOB community composition. It can be only
306 concluded by statistical analysis in this research. Future experimental studies should be conducted to verify
307 the influence of these factors on the AOB diversity index.

308 **4. Conclusions**

309 AOB community dynamics in food waste composting was monitored by PCR-DGGE combined with
310 clone library. The results showed that higher diversity indices of AOB appeared during the mesophilic and
311 cooling phases. In addition, both *Nitrosomonas*-like and *Nitrosospira*-like lineages existed in large amounts
312 in different periods. *Nitrosomonas europaea/eutropha* dominated the thermophilic stage and probably
313 represents a group of bacterium that can adapt to high temperature. Multivariate statistical analysis suggested
314 that nitrate and pH have a predominant effect on AOB community composition in the composting ecosystem.
315 These findings therefore enrich the theory that the relationship between AOB community dynamics and
316 environmental parameters covary. The findings also offer insight into the parameters that control the AOB
317 community dynamics in food waste composting. The results obtained in this study may help lay the
318 foundation to better understand and manage nitrogen cycle in the food waste composting ecosystem.

319 **Acknowledgements**

320 This work was financially supported by the National Environmental Protection Public Welfare Science and
321 Technology Research Program of China (201109024) and International Science & Technology Cooperation
322 Program of China (NO. 2013DFG92600).

323 **References**

- 324 1. R. Zhang, H. M. El-Mashad, K. Hartman, F. Wang, G. Liu, C. Choate and P. Gamble, *Bioresour.*
325 *Technol.*, 2007, 98, 929–935.
- 326 2. J. S. Van Dyk, R. Gama, D. Morrison, S. Swart and B. I. Pletschke, *Renew. Sust. Energ. Rev.*, 2013, 26,
327 521–531.
- 328 3. H. Yu and G. H. Huang, *Bioresour. Technol.*, 2009, 100, 2005–2011.
- 329 4. Z. Li, H. Lu, L. Ren and L. He, *Chemosphere*, 2013, 93, 1247–1257
- 330 5. B. Beck-Friis, S. Smårs, H. Jönsson and H. Krichmann, *J. Agric. Eng. Res.*, 2001, 78, 423–430.
- 331 6. C. Shimaya and T. Hashimoto, *Soil Sci. Plant Nutr.*, 2008, 54, 529–533.
- 332 7. G. A. Kowalchuk and J. R. Stephen, *Annu. Rev. Microbiol.*, 2001, 55, 485–529.
- 333 8. G. A. Kowalchuk, Z. S. Naoumenko, P. J. Derikx, A. Felske, J. R. Stephen and I. A. Arkhipchenko, *Appl.*
334 *Environ. Microbiol.*, 1999, 65, 396–403.
- 335 9. Å. Jarvis, C. Sundberg, S. Milenkovski, M. Pell, S. Smårs, P. E. Lindgren and S. Hallin, *J. Appl.*
336 *Microbiol.*, 2009, 106, 1502–1511.
- 337 10. K. Maeda, S. Toyoda, R. Shimojima, T. Osada, D. Hanajima, R. Morioka and N. Yoshida, *Appl. Environ.*
338 *Microbiol.*, 2010, 76, 1555–1562
- 339 11. G. Innerebner, B. Knapp, T. Vasara, M. Romantschuk and H. Insam, *Soil Biol. Biochem.*, 2006, 38,
340 1092–1100.
- 341 12. N. Yamamoto, K. Otawa and Y. Nakai, *Microbial. Ecology.*, 2010, 60, 807–815.

- 342 13. G. W. Nicol, S. Leininger, C. Schleper and J. I. Prosser, *Environ. Microbiol.*, 2008, 10, 2966–2978.
- 343 14. Y. Okano, R. K. Hristova, C. M. Leutenegger, L. E. Jackson, R. F. Denison, B. Gebreyesus and K. M.
344 Scow, *Appl. Environ. Microbiol.*, 2004, 70, 1008–1016.
- 345 15. L. Racz, T. Datta and R. Goel, *Bioresour. Technol.*, 2010, 101, 6454–6460.
- 346 16. M. P. Bernal, J. A. Albuquerque and R. Moral, *Bioresour. Technol.*, 2009, 100, 5444–5453.
- 347 17. APHA, *Standard Methods for the Examination of Water and Wastewater*, American Public Health
348 Association, Washington, DC, USA, 21nd edn, 2005.
- 349 18. Z. H. Yang, Y. Xiao, G. M. Zeng, Z. Y. Xu and Y. S. Liu, *Appl. Microbiol. Biot.*, 2007, 74, 918–925.
- 350 19. B. Zhang, B. Sun, M. Ji, H. Liu and X. Liu, *Bioresour. Technol.*, 2010, 101, 3054–3059.
- 351 20. G. A. Kowalchuk, J. R. Stephen, W. I. E. T. S. E. De Boer, J. I. Prosser, T. M. Embley and J. W.
352 Woldendorp, *Appl. Environ. Microbiol.*, 1997, 63, 1489–1497.
- 353 21. G. Muyzer, E. C. De Waal and A. G. Uitterlinden, *Appl. Environ. Microbiol.*, 1993, 59, 695–700.
- 354 22. C. E. Shannon and W. Weaver, *The Mathematical Theory of Communication*. University of Illinois
355 Press, Urbana, 1963.
- 356 23. J. Zhang, G. Zeng, Y. Chen, M. Yu, Z. Yu, H. Li, Y. Yu and H. Huang, *Bioresour. Technol.*, 2011, 102,
357 2950–2956.
- 358 24. Yu, H., Zeng, G., Huang, H., Xi, X., Wang, R., Huang, D., Huang, G., Li, J., *Biodegradation*, 2007, 18,
359 793–802.
- 360 25. S. Smårs, L. Gustafsson, B. Beck-Friis and H. Jönsson, *Bioresour. Technol.*, 2002, 84, 237–241.
- 361 26. C. Liang, K. C. Das and R. W. McClendon, *Bioresour. Technol.*, 2003, 86, 131–137.
- 362 27. S. Malchair, H. J. De Boeck, C. M. H. M. Lemmens, R. Ceulemans, R. Merckx, I. Nijs and M. Carnol,
363 *Appl. Soil. Ecol.*, 2010, 44, 15–23.
- 364 28. L. Wittebolle, N. Boon, B. Vanparrys, K. Heylen, P. De Vos and W. Verstraete, *J. Appl. Microbiol.*, 2005,

- 365 99, 997–1006.
- 366 29. A. P. Trzcinski, M. J. Ray and D. C. Stuckey, *Bioresour. Technol.*, 2010, 101, 1652–1661.
- 367 30. J. Lepš, and P. Šmilauer, *Multivariate Analysis of Ecological Data Using CANOCO*. Cambridge
368 University Press, Cambridge, UK, 2003, 43–75.
- 369 31. S. J. Kemmitt, D. Wright, K. W. Goulding and D. L. Jones, *Soil Biol. Biochem.*, 2006, 38, 898–911.
- 370 32. W. De Boer and G. A. Kowalchuk, *Soil Biol. Biochem.*, 2001, 33, 853–866.
- 371 33. R. A. Nugroho, W. F. M. Röling, A. M. Laverman and H. A. Verhoef, *Microb. Ecology.*, 2007, 53, 89–
372 97.
- 373 34. M. J. Frijlink, T. Abee, H. J. Laanbroek, W. De Boer and W. N. Konings, *Arch. Microbiol.*, 1992, 157,
374 194–199.
- 375

376 **Figure legends:**

377

378 **Fig. 1** Schematic of the lab-scale composting reactor

379

380 **Fig. 2** Variation of (a) temperature and pH, (b) organic matter content and moisture content, and (c)
381 ammonium and nitrate in the food waste composting for 15 days. The bars represent the standard deviations
382 of the mean values ($n = 3$).

383

384 **Fig. 3** DGGE profile of AOB generated by nested PCR-DGGE. Labels along the bottom indicate the
385 composting days; (A) DGGE profile; (B) diagram of sample lanes.

386

387 **Fig. 4** Neighbor-joining tree with Kimura 2-parameter substitution of partial 16S rRNA gene sequences of
388 AOB DGGE bands in this study and from NCBI GenBank database. Bootstrap values ($> 50\%$) are indicated
389 at branch points. The scale bar represents 1% sequence divergence.

390

391 **Fig. 5** Distance triplot of the redundancy analysis on the AOB community composition and environmental
392 parameters during food waste composting. Composting environmental parameters are indicated by solid lines
393 with filled arrows. AOB communities are shown using gray dotted lines with unfilled arrows. Samples are
394 represented by solid circles and sample numbers refer to the sampling days.

Table 1 Physicochemical characteristics of the initial raw materials with standard deviation

Parameter	Food waste	Mushroom residue
Moisture content (% <i>WW</i>)	74.06 ± 2.81	11.87 ± 0.34
pH	6.08 ± 0.01	7.63 ± 0.02
EC (mS cm ⁻¹)	8.90 ± 0.34	2.50 ± 0.51
Organic matter (% <i>DW</i>)	91.43 ± 0.09	82.97 ± 0.52
Total C (% <i>DW</i>)	47.11 ± 0.04	42.79 ± 0.26
Total N (% <i>DW</i>)	2.73 ± 0.11	0.23 ± 0.01
C/N ratio	17.26	186.04

Mean and standard error are shown ($n = 3$), *WW* wet weight, *DW* dry weight

Table 2 AOB band number and Shannon diversity index (H) of the DGGE profiles for each compost sample

Index	Days of composting					
	1 d	3 d	6 d	9 d	12 d	15 d
Band number	6	6	4	3	8	4
Shannon diversity index (H)	1.63	1.49	1.32	0.89	1.85	1.04

Table 3 Redundancy analysis results of the AOB DGGE profiles

Axes	Axis 1	Axis 2	Axis 3	Axis 4	Total variance
Eigenvalues	0.411	0.288	0.170	0.042	1.000
Species-environment correlations	0.997	0.998	0.999	0.777	
Cumulative percentage variance of species data	41.1	69.9	86.8	91.0	
Cumulative percentage variation of species-environment relation	45.1	76.8	95.4	100.0	
Sum of all eigenvalues					1.000
Sum of all canonical eigenvalues					0.910

Monte Carlo significance tests for AOB data: sum of all Eigen values, 1.000; significance of first canonical axis, F value = 4.880, p = 0.002; significance of all canonical axes, F value = 17.688, p = 0.002. F and p values were estimated using Monte Carlo permutations.

Table 4 Eigenvalues, *F* values, and *P* values obtained from the partial RDA testing the influence of the significant parameters on the AOB community

Parameters included in the model	Eigenvalues	% Variation explains solely	<i>F</i> value	<i>p</i> value
Nitrate	0.273	27.3	3.751	0.012
pH	0.217	21.7	2.774	0.024
All the above together	0.547	54.7	5.439	0.002

Partial RDA based on Monte Carlo permutation ($n = 499$) maintained only the significant parameters in the models. For each partial model, the other significant parameter was used as a covariable. *F* and *p* values were estimated using Monte Carlo permutations. The sum of all eigenvalues for the partial RDA was 1.000.

Fig. 1

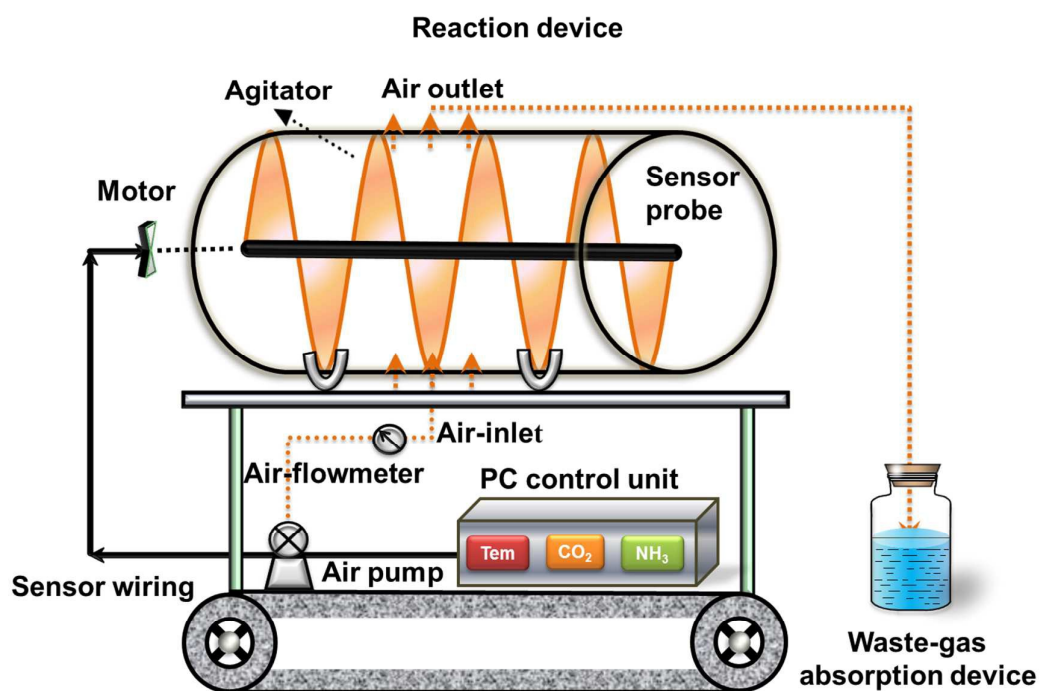


Fig. 2

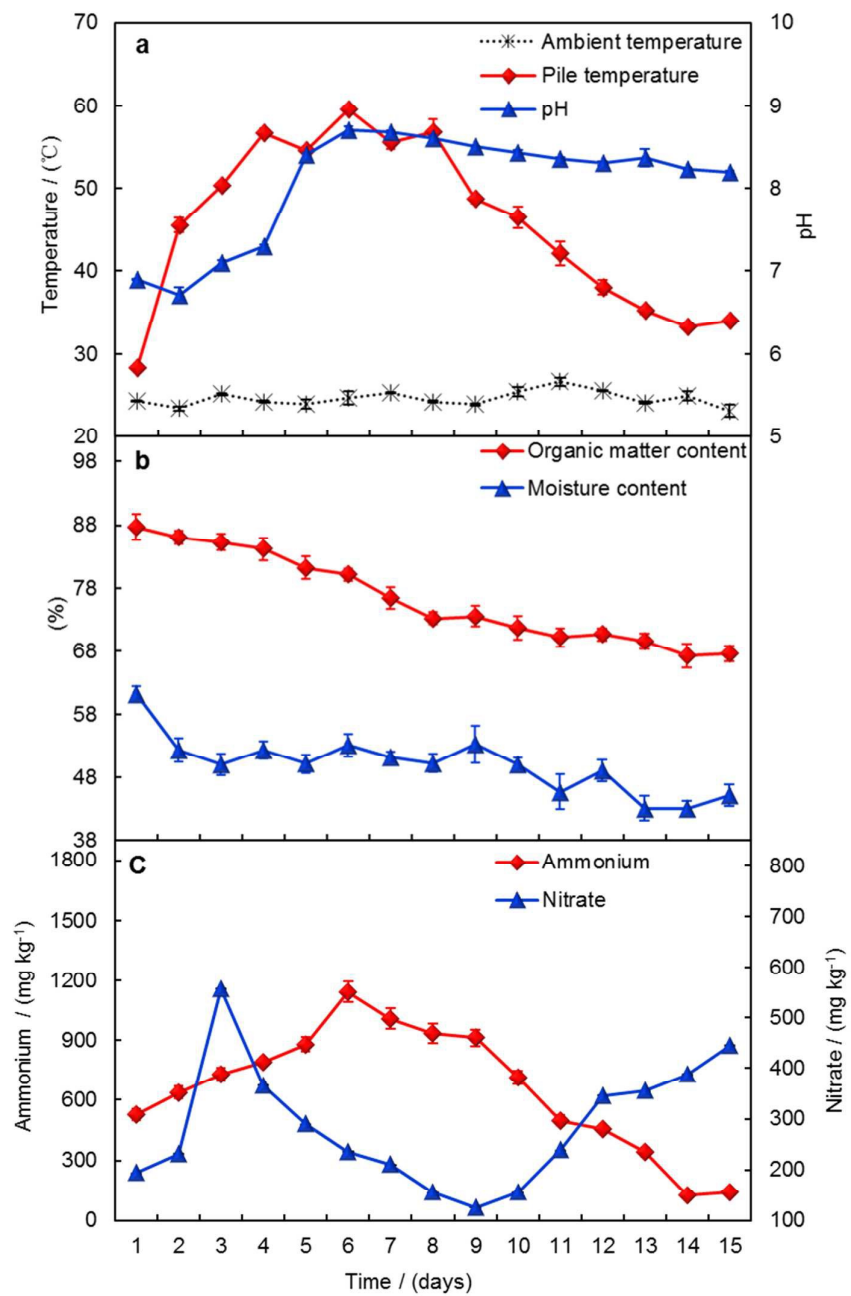


Fig. 3

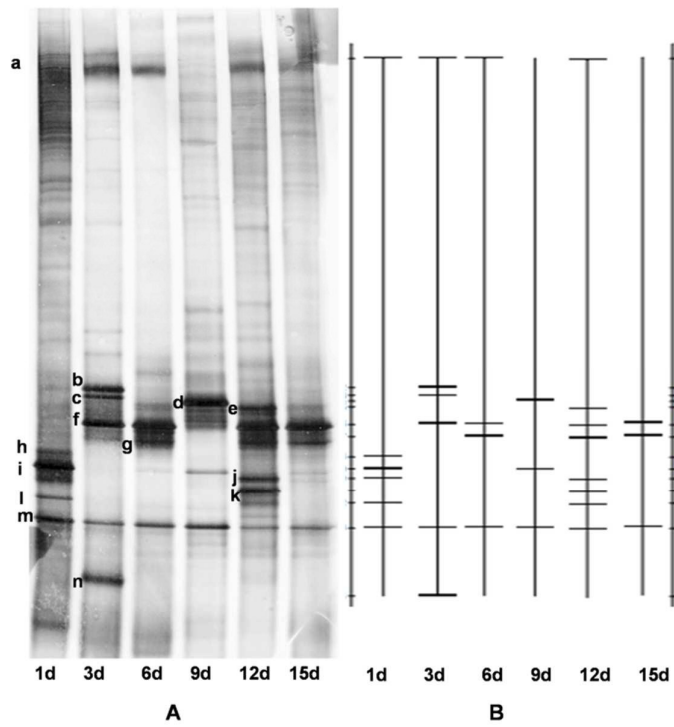


Fig. 4

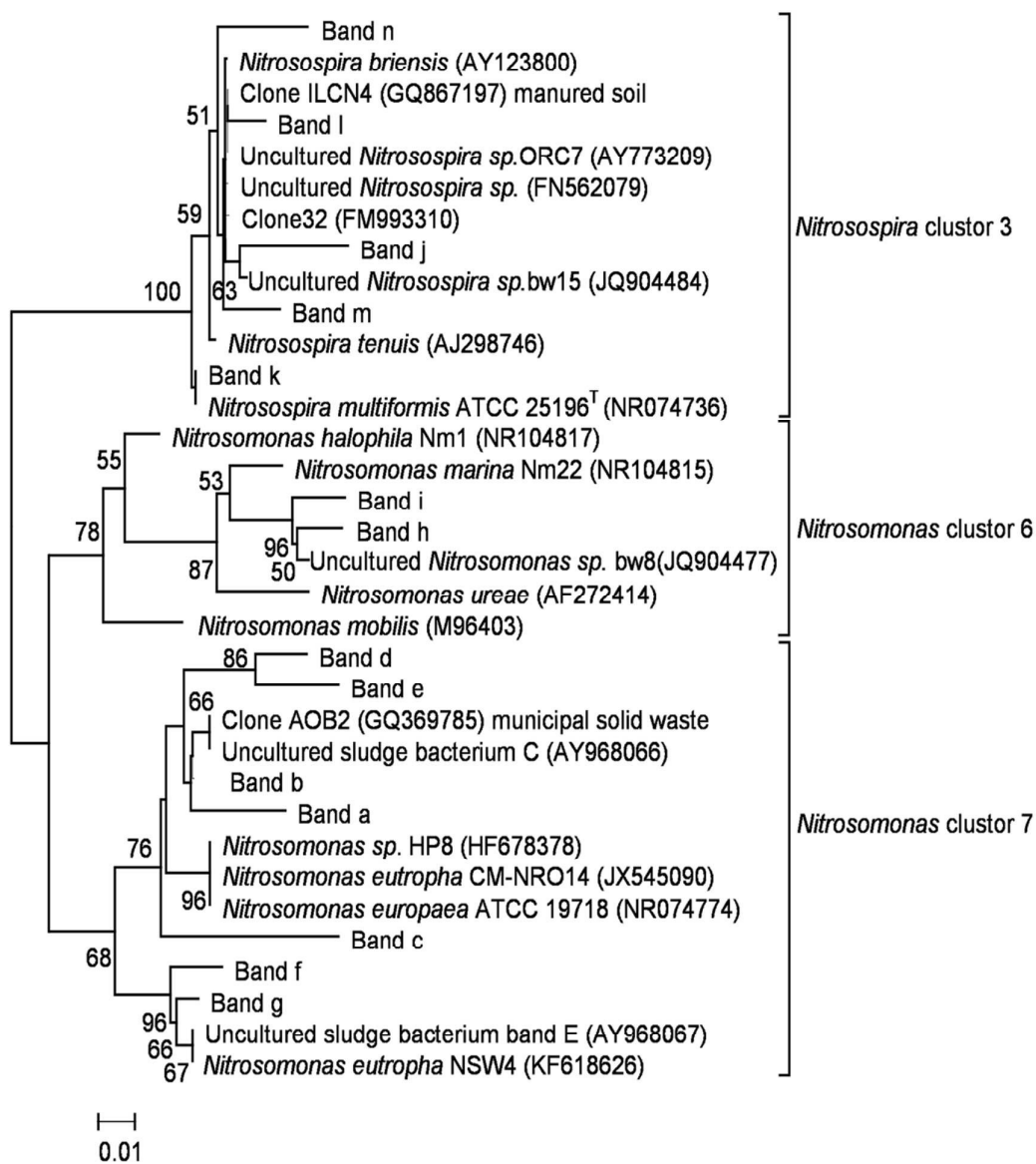
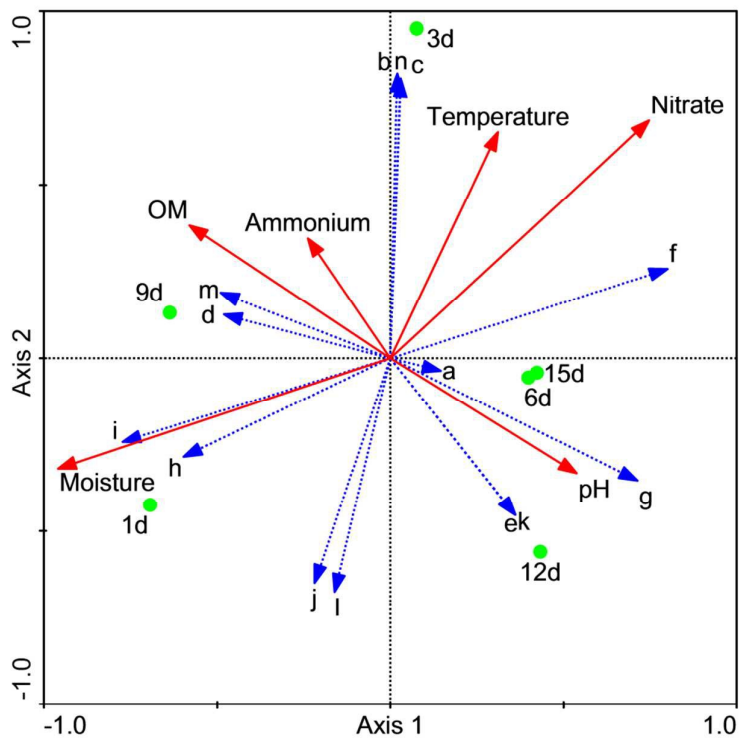


Fig. 5



Graphical abstract

This paper aimed to identify and prioritize some environmental parameters that affect AOB community composition during food waste composting.

